REVISTA IBRACON DE ESTRUTURAS E MATERIAIS
IBRACON STRUCTURES AND MATERIALS JOURNAL

Potentialities of infrared thermography to assess damage in bonding between concrete and GFRP

Potencialidades da termografia infravermelha na avaliação de danos na aderência entre concreto e PRFV

M. M. CALDEIRA [a]
marimartino@gmail.com

I. J. PADARATZ [b]
padaratz@gmail.com

Abstract

This paper demonstrates the application of the active infrared thermography to detect damage in bonding between concrete and glass fiber reinforced polymer (GFRP). Specimens of concrete and mortar with GFRP externally bonded were prepared and at their interfaces were inserted polystyrene discs to simulate damages. The samples were divided into two groups. In group 1, one sample was correctly bonded by a GFRP plate to the concrete, but in the other three were inserted polystyrene discs which had different diameters to simulate damages in bonding. In group 2, all of the samples contained identical polystyrene discs at their interfaces, but the total thickness of each specimen was different, because the objective was to evaluate the ability of the camera to capture the simulated damage in depth. The experimental procedure was divided into two stages. In the first stage, four types of heating were used to heat samples of group 1: incandescent lamp, kiln, blended lamp and fan heater. Thus, it was possible to detect the damage and to observe its format and length. It was noticed that the infrared images are different depending on the heat source incident on the specimen. Therefore, group 2 was tested only for the more efficient heating (incandescent lamp). In the second stage, the infrared equipment was tested. Some of the parameters that must be inserted in the camera were varied in order to understand their influence on image formation. The results show the effectiveness of infrared thermography to assess adherence in GFRP/concrete interface. In the present work, the best results were obtained when the image is captured towards GFRP/concrete and using incandescent lamp. It was observed that the image and measured temperature suffer significant distortion when a false value was inserted for the parameter emissivity.

Keywords: infrared termography, non destructive test, concrete, frp, debonding.

Resumo

Para demonstrar a potencialidade da aplicação da técnica da termografia infravermelha ativa para detecção de danos na aderência entre concreto e polímero reforçado com fibra de vidro (PRFV), são utilizados neste trabalho corpos de prova de concreto e argamassa colados externamente com PRFV, em cuja interface foram inseridos discos de EPS (poliestireno expandido) para simular danos. Os corpos de prova foram divididos em dois grupos. No grupo 1, em uma das amostras, a chapa de PRFV estava totalmente aderida ao concreto, nas outras três foram inseridos discos de EPS de diferentes diâmetros para simulação de regiões com falha de aderência. No grupo 2, todos os corpos de prova continham idênticos discos de EPS na interface, porém a espessura total de cada corpo de prova era diferente, pois o objetivo foi avaliar a capacidade da câmera em alcançar o dano simulado. O procedimento experimental dividiu-se em 2 etapas. Na primeira, foram utilizados 4 tipos de aquecimento para o grupo 1: lâmpada incandescente, estufa, lâmpada de mercúrio de alta pressão e termoventilador. Assim, foi possível detectar o dano e observar seu formato e extensão. Notou-se uma diferenciação das imagens devido à fonte de calor incidente no corpo de prova e por isso, o grupo 2 foi testado apenas para o aquecimento mais eficiente (lâmpada incandescente). Na segunda etapa, a câmera termográfica foi posta em evidência. Alguns dos parâmetros de ajuste que devem ser nela inseridos foram variados a fim de entender suas influências na formação da imagem e consequentemente na identificação do dano. Os resultados revelam a eficiência da termografia infravermelha para avaliar a aderência na interface concreto/PRFV. Neste trabalho, os melhores resultados foram obtidos quando a imagem foi captada para uma amostra aquecida no sentido PRFV/Concreto por lâmpada incandescente e para quando são inseridos na câmera infravermelha os parâmetros corretos, especialmente a emissividade térmica.

Palavras-chave: termografia infravermelha, ensaios não destrutivos, concreto, polímero reforçado com fibras, danos na aderência.

[a] Programa de Pós-graduação em Engenharia Civil (PPGEC), Universidade Federal de Santa Catarina (UFSC), Florianópolis-SC, Brasil;
[b] Departamento de Engenharia Civil, Universidade Federal de Santa Catarina (UFSC), padaratz@gmail.com, Florianópolis-SC, Brasil.

1. Introduction

The combination of Glass Fibres Reinforced Polymer (GFRP) and concrete has gained increasingly attention in Civil Engineering by joining lightness and strength [1]. This application has been especially used as structural reinforcement.[2].

One of the main factors that influence the total strength of this arrangement is the correct adherence of the interface between these two materials once the right connection between FRP and concrete allows they work as an unit. [3]. Therefore, quality of interface adherence is needed and if a flaw is detected it must be localized and characterized[4].

A defect caused by incorrect adherence of FRP can only appear after bonding the polymer to a concrete surface. So, in order to detect flaws, the inspection has to identify it through the FRP. A quick, practical and possible solution is the use of a non destructive test known as infrared thermography [5][6].

Thus, the main objective of this paper is the evaluation of defects at FRP/concrete interface using the active infrared thermography. To do this, a qualitative analysis will be used and it will compare different thermal excitations and different defect positions (related to depth). Also, the behaviour of the thermal images will be evaluated when the infrared camera parameters are not correctly adjusted.

Related to this topic, there is still a lack of research and so this paper intends to contribute to new experimental results and also compare them to previous works.

2. Infrared thermography and detection of defects at FRP/concrete interface by thermal excitation

There are already researches that present the infrared thermography as an efficient technique to evaluate defects at FRP/Concrete interface. One of them[7] uses water and air-filled debonds in different sizes. These simulated flaws were placed underneath the layer of the polymer and then samples were heated by two quartz tower heaters for 70 seconds. Some minutes after heating the images were captured. The results present the artificial defects quite evidently (shown up as "hot-spots") when the thermal images were analysed. So, the effectiveness of the method was proved.

Another paper [8] analyses different types of artificial flaws such as: timber, steel, Teflon and cork. The tests were performed considering two types of thermal excitation. Firstly, two photographic flashes were used adopting a duration pulse of 10 milliseconds and the frequency was set to 22Hz. Afterwards, two halogen lamps were used and they heat the area for 10, 30 and 60 seconds. Comparing the types of heating, the thermal contrast is not evident when the thermal excitation is made by short pulses. According to the authors, this could be improved if the sample surface had a more homogeneous thermal emissivity. On the other hand, heating an area using the halogen lamps showed a better contrast in the infrared image because, in this case, more thermal energy was provided to the sample's surface, if compared to the previous thermal excitation.

Another experimental work [9] evaluates different types of thermal excitation when applied infrared thermography. In this case, individual samples of composite material were subjected to infrared thermography in order to detect internal damages when exposed to impact. It was concluded that the convective heating presents

more effective results than incandescent lamps.

Like other scientific works previously cited, it is possible to notice the importance of choosing the type of heating when active infrared thermography inspections are performed in FRP, and therefore this is one of the issues which will be discussed in the present paper.

3. The thermal image formation and the influence of the inserting parameters in the infrared camera

The influence of the parameters which have to be inserted in the infrared camera is another important factor which also interferes in the infrared image formation, once these are the data that allow the temperature calculation and the adjustment of thermal image [10]. Thus, it is necessary to understand how this equipment works in order to study its calibration parameters.

The infrared camera is restricted to the infrared spectral band and its operation is based on the detection of infrared radiation emitted by bodies which forms "thermal images". This camera detects exclusively radiant thermal energy from bodies' surfaces, so it does not detect the reflected visible light, which means that the thermal images can be obtained even in total darkness.

If the camera is pointed to an object, it receives emitted radiation from the object's surface and from the environment adjacent to the body. Both are attenuated by atmosphere before they reach the camera. The camera receives also a third contribution: radiation emitted from the atmosphere, as Figure 1 illustrates.

Figure 1 illustrates the total radiation potency that the camera receives (Wtot).

So:

$$W_{tot} = \varepsilon \tau \, W_{obj} + (1 - \varepsilon) \, \tau \, W_{refl} + (1 - \tau) \, W_{atm} \qquad (1)$$

Wtot: Total potency [W]
Wobj: Potency of radiation emitted by object [W]
Wrefl: Potency of radiation emitted by adjacent environment [W]
Watm: Potency of radiation emitted by atmosphere [W]
ε : Object's emittance [no unity]
τ: Atmosphere transmittance [no unity]

So, in order to better analyse the infrared thermography inspections when considered defects at FRP/concrete interface, it is necessary to study some parameters which are inserted in the infrared camera such as: thermal emissivity, distance from the lens to the object, and temperature and humidity of the environment.

In relation to this subject, scientific works are more focused on evaluation of thermal emissivity. One of these works [11] surveyed about what would be the best technique of thermal emissivity measurement. The paper calls attention to the uncertainty of thermal emissivity tabulated values because they are not often valid for insertion into infrared camera. Another important point considered in this study was the accuracy of emissivity measurement once it can affect the precision of thermal measurement. Other author [12], has observed that thermal emissivity is one of the main reasons why theoretical and experimental results do not coincide when considered defects in ceramic materials applying the infrared thermography method.
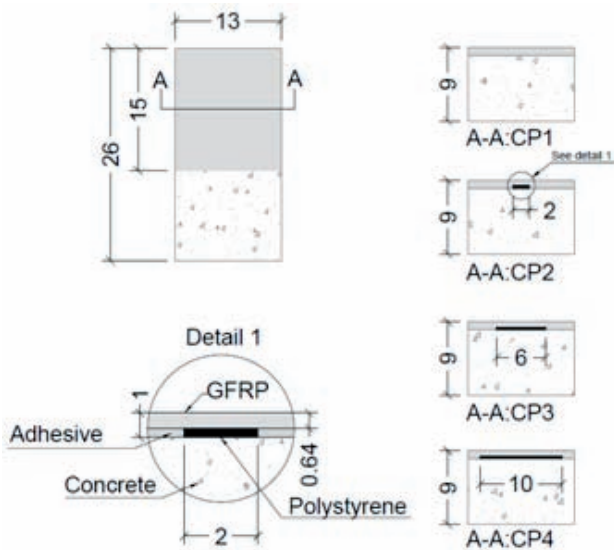
Figure 1 – Schematic representation of a thermographic measurement. 1) adjacent ambient, 2) object, 3) atmosphere, 4) camera. Tobj: object's temperature, Trefl: reflected temperature, Tatm: atmosphere temperature (room temperature). Wobj: radiation potency emitted by object, Wrefl: radiation potency emitted by adjacent ambient, Watm: radiation potency emitted by atmosphere (17)
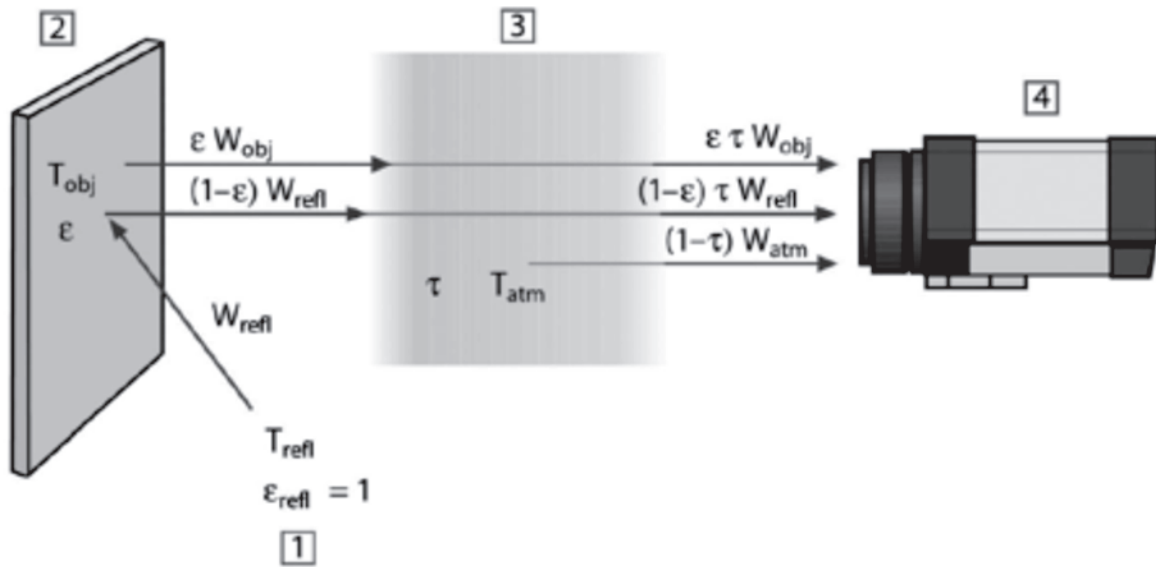
The scientific works previously cited demonstrate the relevance of the study of the parameters that must be inserted into the infrared camera. However, it is noteworthy that, despite the extensive literature research carried out, no parametric studies of these parameters were found and so this is one of the purposes of this work. Therefore, this article presents also an unprecedented contribution to the study of the parameters to be inserted into the infrared camera, assisting in the extension and deepening of this subject.

4. Materials and experimental program

4.1 Characteristics of the samples

Samples were divided in two different groups: group 1 and group 2. Group 1 consists of four concrete samples whose dimensions were 26.0 x 13.0 cm and 9.0 cm of thickness. In one of the faces of the samples a GFRP sheet (15.0 x 13.0 cm and 0.635 cm of thickness) was adhered by epoxy resin. Only in one sample of group one, the GFRP sheet was totally adhered to the concrete whereas in the remaining three thin polystyrene discs were inserted underneath the GFRP sheet to simulate a debonding. These discs had different diameters for each sample: 2, 6 and 10 cm.

Group two consists of six samples of 15.0 x 13.0 cm. Each sample had different thicknesses: 7, 6, 5, 4, 3 and 2 cm. A GFRP sheet of 15.0 x 13.0 and 0.635 cm of thickness was bonded at one of the samples surface. All of them had a thin polystyrene disc of 3 cm diameter underneath GFRP sheet as shown in Figure 3.

An epoxy resin was applied to bond the GFRP to the concrete surface, except in the area of the polystyrene disc. All samples were at an age greater than 180 days when tested and at this age the heat of hydration does not influence their temperatures [13].

Figure 2 – Samples of group 1 (measurement in cm)

Figure 3 – Samples of group 2 (measurement in cm)
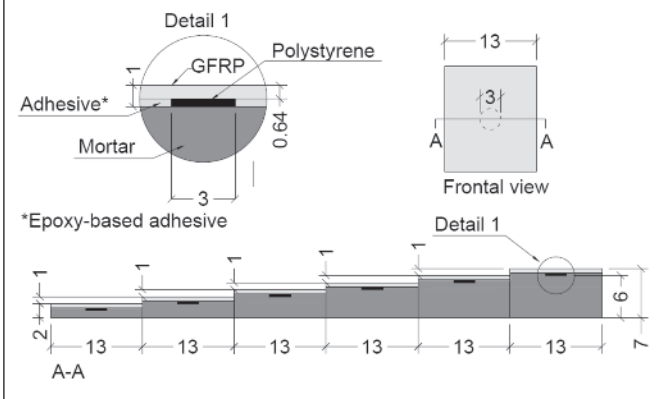
4.2 Samples heating

Before capturing infrared images, samples were subjected to previous heating. The type of heating was: kiln, incandescent lamp (200 Watts), high-pressure sodium lamp (250 Watts) and convection heater (1500 Watts).

Samples were placed in kiln for 24 hours at 32° C. However, considering the heating by lamp (incandescent lamp or high-pressure sodium lamp) the front surface of samples was positioned perpendicular to the lamp, which was 12 cm above the sample, for 5 minutes. The convection heater was placed 14 cm from the front face of the specimen which was heated for 6 minutes. It is important to note that the convection heater was not perpendicular to the central point of simulated damage because the heat concentration

does not occur in the centre of the appliance. For each new heating, a rest period of 24 hours was provided so that the specimens could reach a thermal equilibrium condition with the ambient and thus they could be subjected again to another heating heat source. In group 1, infrared images were captured towards GFRP-concrete, but in group two, images were captured towards concrete-GFRP, one minute after removing the heat source in both cases.

After testing the different types of heating to group one, results showed that when samples were heated by incandescent lamp, the best infrared images were obtained. So, this kind of heating was used to test samples of group two.

An infrared camera was used to capture the images. This device was a FLIR B400, specific for inspection buildings, available on Non Destructive Research Group (GPEND) at Federal University of Santa Catarina.

4.3 Parameters of infrared camera

In order to evaluate the parameters which must be inserted in the camera, the samples of group one were used and they were heated by incandescent lamp. In this case, the temperature and humidity of the environment were set according to the weather forecast of Florianópolis –SC, Brazil, on the day and time of the experiment, as shown in Table 1. In order to calibrate thermal emissivity, the procedures recommended by the camera manufacturer's manual were adopted.

As thermal emissivity of materials considered in this experiment are height and the ambient is not subjected to strong heat sources, the parameters of "Reflected Apparent Temperature" does not influence the final result and so it does not need to be set. The value inserted was 20°C.

Table 1 also shows the measured values of the parameters, i.e. the values of ambient temperature, humidity, distance from lens to object and emissivity which were obtained in the moment of the experiment. The measured values are named "real values" or "real parameters".

Afterwards, the variation of parameters which will be inserted in the camera was defined so that the difference between images (or temperatures) captured when included real or false parameters could be observed.

Tables 2 to 5 present how the parameters were varied and which were the values inserted in the camera, for each case. It was noted that the distance from lens to object is the only parameter which can be varied considering the "real value", and so two different distances were adopted: 1m and 5 m.

While one parameter was varied, the other parameters were set to the real measurements. In case of distance from lens to object the standard adopted was 1 m distance.

Table 1 – Real values (or measured values) of parameters

Parameters	Measured values
Temperature	17°C
Relative air humidity	64%
Thermal emissivity	0.96
Distances lens-object	1m
	5m

Table 2 – Real value and variations of room temperature

Room temperature (°C)					
Variations					
0%	30%	60%	100%	150%	200%
17	22.1	27.2	34.0	42.5	51.0

Table 3 – Real value and variations of thermal emissivity

Thermal emissivity			
Variations			
0%	-30%	-60%	-90%
0.96	0.7	0.4	0.1

Table 4 – Real value and variations of relative air humidity				
Relative air humidity (%)				
Variations				
0%	+30%	-30%	-60%	-90%
64	83	45	26	6

Table 5 – Real values and variations of distance lens-object				
Distance lens-object (m)				
Real	Variations			
0%	+30%	-30%	-60%	-90%
1	2	5	10	15
5	1	2	10	15

The infrared images were captured for each sample of group 1, for each variation of parameter, after being heated by incandescent lamp located 12 cm distant from the surface sample, for 5 minutes. In this case, a special function of the camera which allows the measurement of one point in the image was used. The chosen point was the centre of the artificial defect.

If one parameter is varied, it is expected a different result (or a different infrared image). However, a careful analysis is needed because when the heating stops the natural tendency is that the temperature of the sample decreases to reach the thermal equilibrium. Thus, the analysis must not consider this decrease as an error caused by the insertion of false parameter. To solve this problem, the capture of infrared images followed the next sequence: firstly, images were captured when inserted real parameters, then images were captured setting false parameters and finally images were captured again when inserted the real parameters.

Despite the short period of time between the first and the second measurement (less than 1 minute), the sample still loses heat because of its thermal properties. So, recording the infrared image using real parameters twice (first and last image recorded) indicates whether the decrease of temperature is related to the setting of parameters or not.

Scientific studies already proves the efficiency of infrared thermography to detect flaws at FRP/concrete interface[14][15][16]. How-

ever, this article analyses this subject even deeper providing results of an assessment for different types of heating and evaluates the infrared image for different situations, as it will be shown next.

5. Results and discussion

5.1 Samples of group 1

The infrared images captured for samples of group 1, after heating using incandescent lamp (Figures 4 to 7), show clearly the location and shape of the artificial defect. It is important to note that the difference of temperature between the location of the defect and the sound area increases as the defect becomes greater.

When the kiln was used to heat the same samples, it was not so easy to observe the defects in infrared images and so, two special camera functions named "above" and "below" were used. At the moment the samples were removed from kiln two images were captured: the first one shows in infrared only temperatures above the temperature marked in the white square (on the right of image) and the second one present the lower temperatures, as shown in Figures 8 to 15. In this case, the defect is visible, but not as visible as when samples were heated by incandescent lamp.
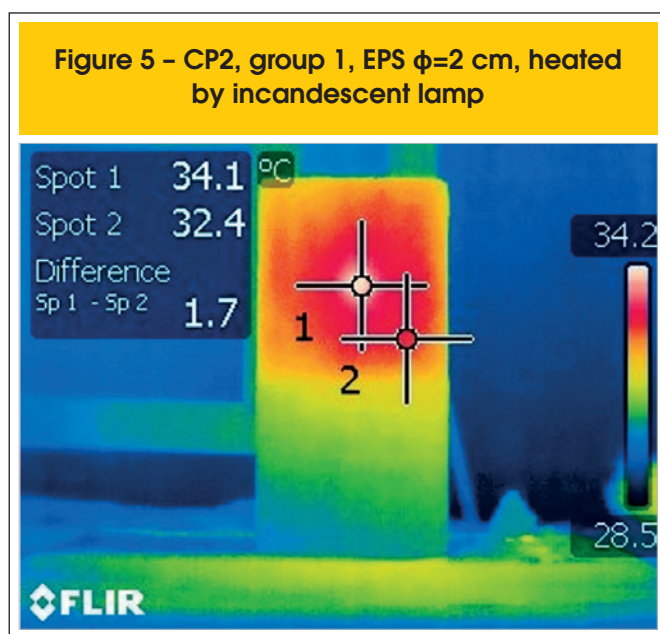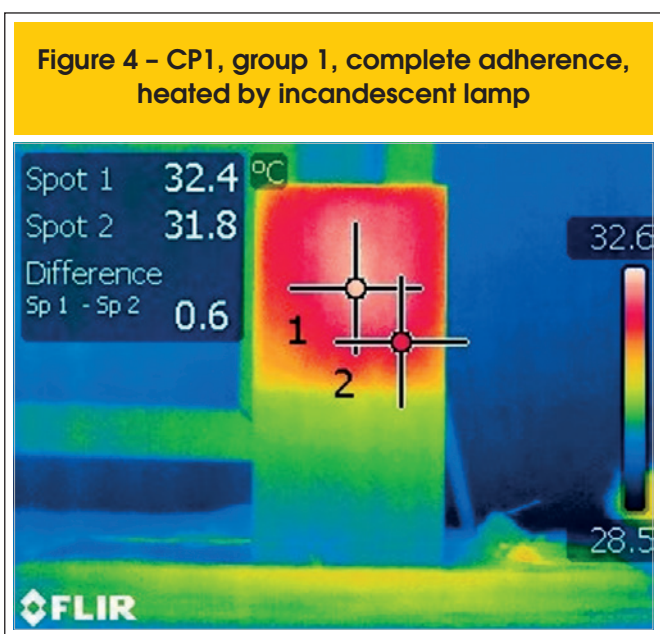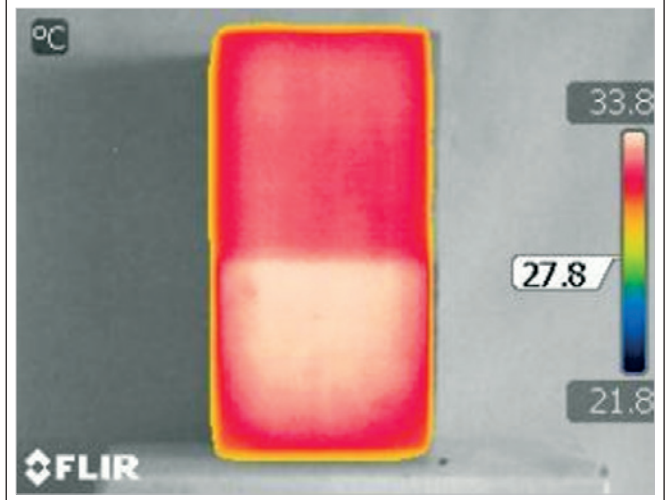

Figure 4 – CP1, group 1, complete adherence, heated by incandescent lamp

Figure 5 – CP2, group 1, EPS ɸ=2 cm, heated by incandescent lamp

Figure 6 – CP3, group 1, EPS φ=6 cm, heated by incandescent lamp

Figure 8 – CP1, group 1, complete adherence, kiln, higher temperatures (function "above")

The results shown in Figures 16 to 19 are related to heating samples using the convection heater.

The convection heater could rise even more the temperature of samples and this means that the defect can be clearly visible. Nonetheless, the heating was not uniform and this can induce to mistaken interpretation of results. For example, it is possible to conclude that there is a defect in the bottom left of CP1 (Figure 16). The other images also present higher temperatures in the top left corner which could be wrongly interpreted as a small defect. So, the conclusion is that the larger the defect is, if the convection heater is correctly positioned, the better the result is. Figures 18 and 19 prove this affirmation once the polystyrene contour disc appears clearly and the heat build-up in the upper left side is less visible.

Finally, the results of experiments using high-pressure sodium lamp are shown in Figures 20 to 23.

In this case, the difference of temperature between the place where the defect is and the sound area is small, but it increases when the defect dimension increases. Furthermore, as the emission of heating is not high, the image loses some clearness, if compared to the images obtained for the other heat sources studied.

Comparing the four heating sources used in samples of group 1, it was observed a better resolution when images were captured after being heated by incandescent lamp. Thus, only this heating device was applied on samples of group 2, as the main aim next is to work out how deep it could be reached by the infrared camera to detect the defect.

Figure 7 – CP4, group 1, EPS φ=10 cm, heated by incandescent lamp

Figure 9 – CP1, group 1, complete adherence, kiln, lower temperatures (function "below")
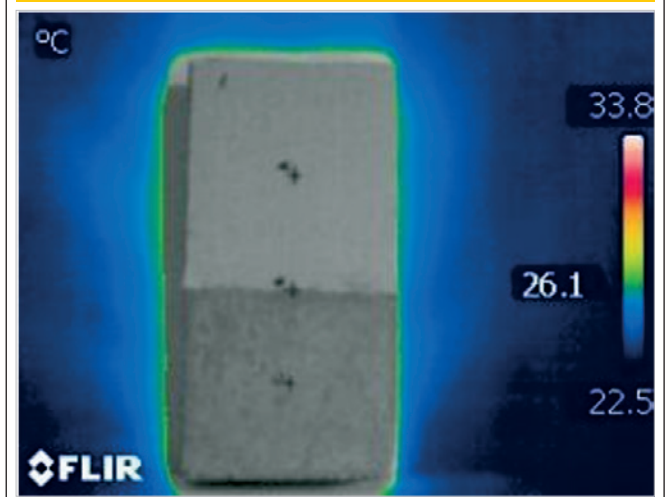
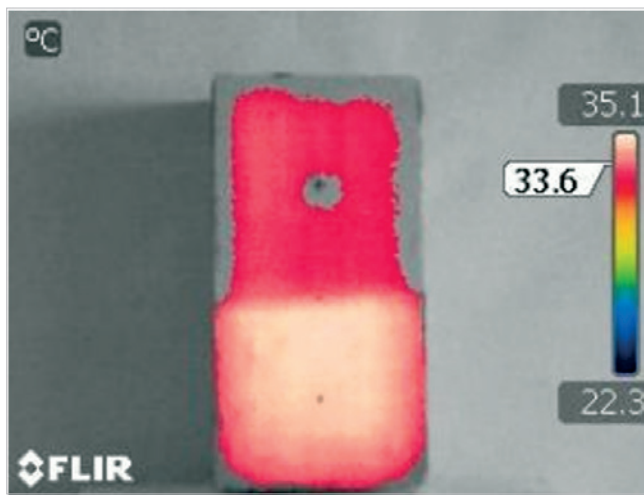Figure 10 – CP2, group1, EPS φ=2 cm, kiln, higher temperatures (function "above")

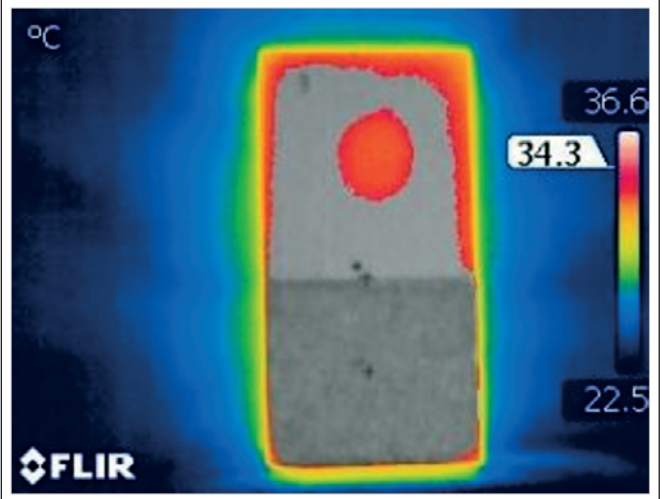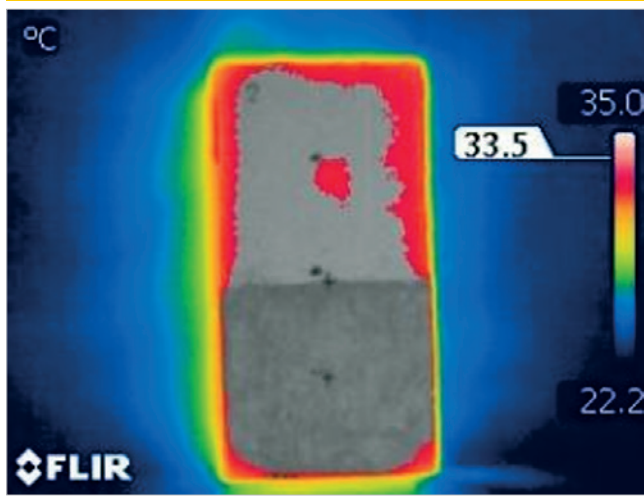Figure 11 – CP2, group 1, EPS φ=2 cm, kiln, lower temperatures (function "below")

Figure 12 – CP3, group1, EPS φ=6 cm, kiln, higher temperatures (function "above")

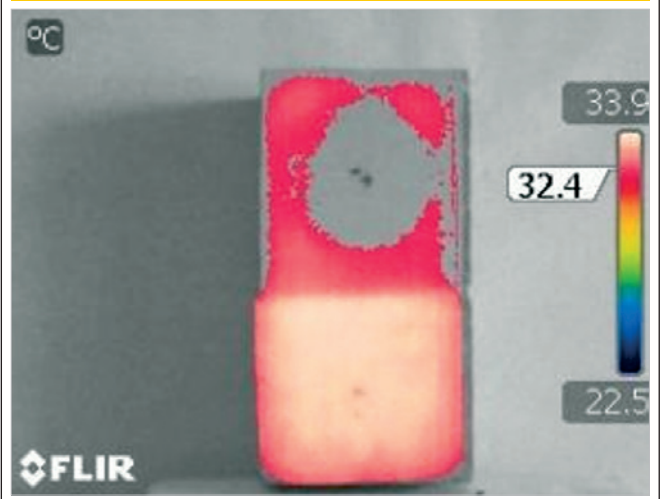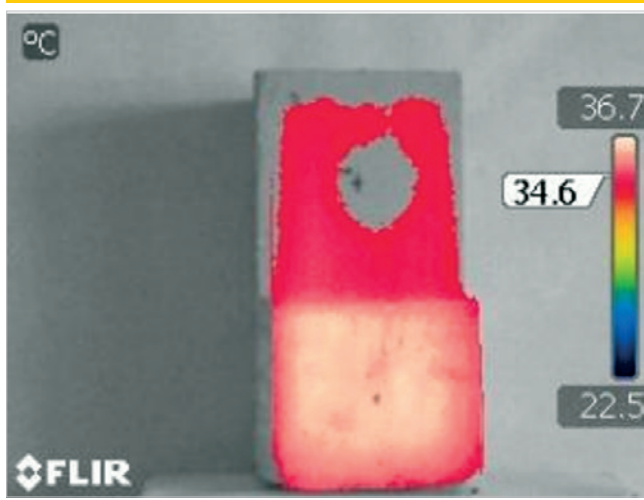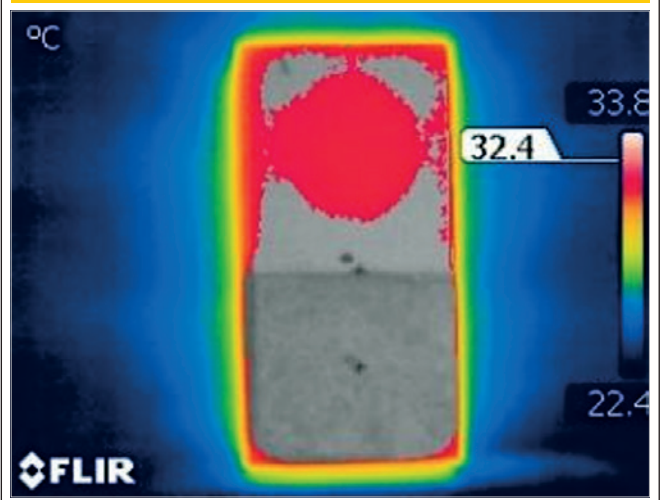Figure 13 – CP3 group1, EPS φ=6 cm, kiln, lower temperatures (function "below")

Figure 14 – CP4, group1, EPS φ=10 cm, kiln, higher temperatures (function "above")

Figure 15 – CP4, group1, EPS φ=10 cm, kiln, lower temperatures (function "below")

Figure 16 – CP1, group 1, complete adherence, heated by convection heater

Figure 17 – CP2, group 1, EPS ɸ=2cm, heated by convection heater

Figure 18 – CP3, group 1, EPS ɸ=6 cm, heated by convection heater

Figure 19 – CP4, group 1, EPS ɸ=10 cm, heated by convection heater

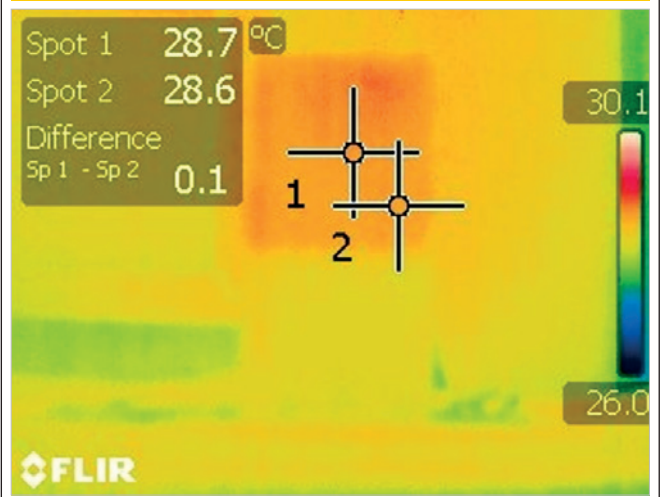**Figure 20 – CP1, group 1, complete adherence, heated by high-pressure sodium lamp**
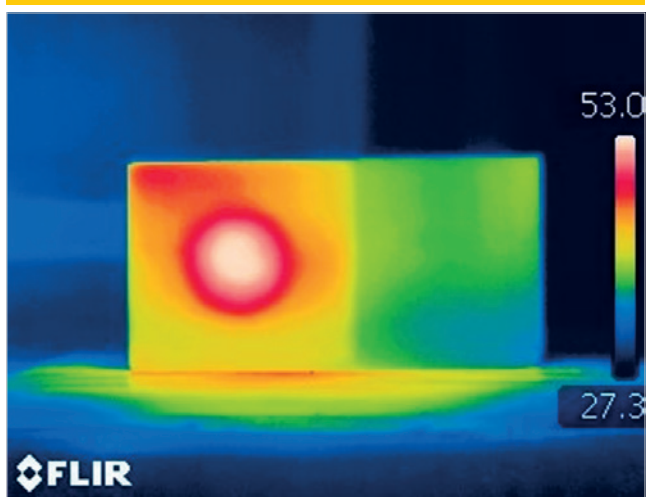

Figure 21 – CP2, group 1, EPS ɸ=2 cm, heated by high-pressure sodium lamp

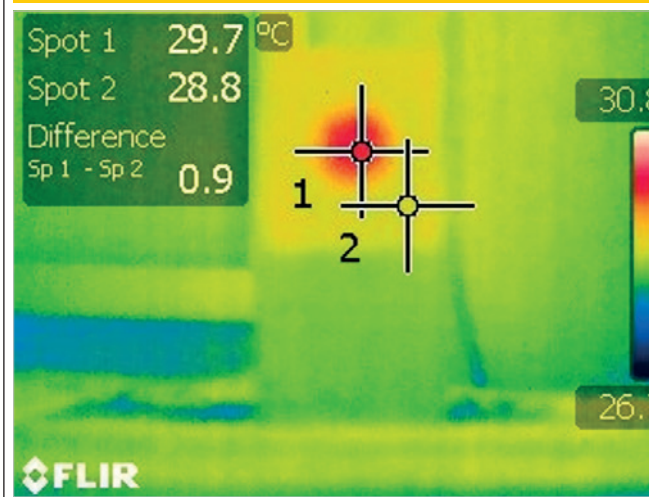Figure 22 – CP3, group 1, EPS φ=6 cm, heated by high-pressure sodium lamp
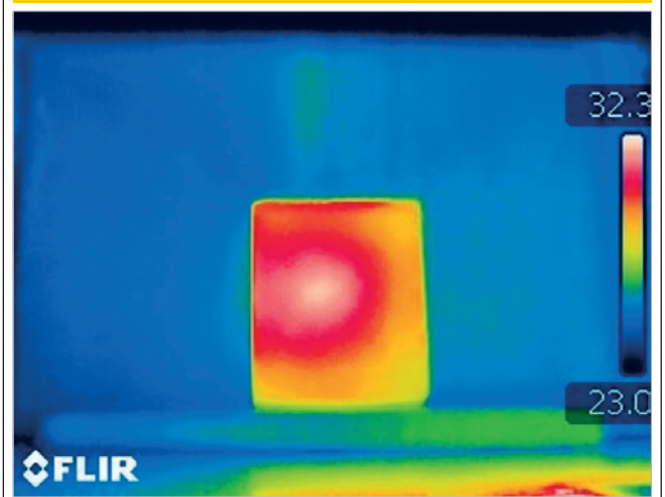

Figure 25 – CP2, group 2, height 3 cm

Figure 23 – CP4, group 1, EPS φ=10 cm, heated by high-pressure sodium lamp

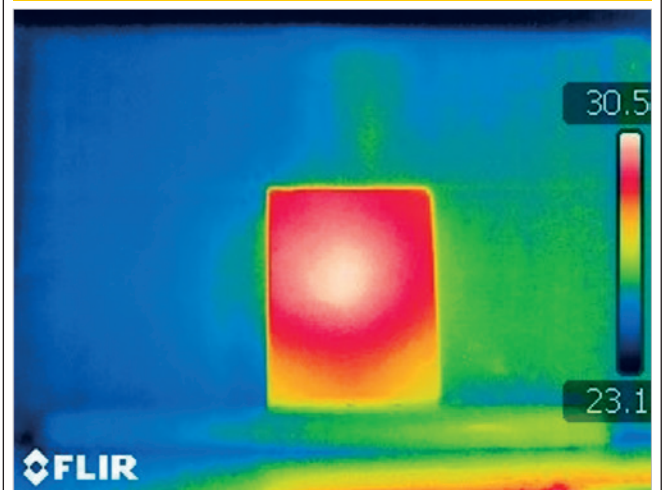Figure 26 – CP3, group 2, height 4 cm

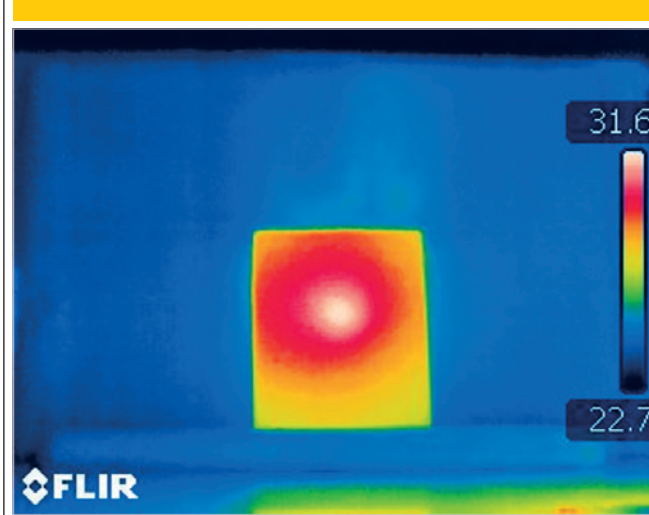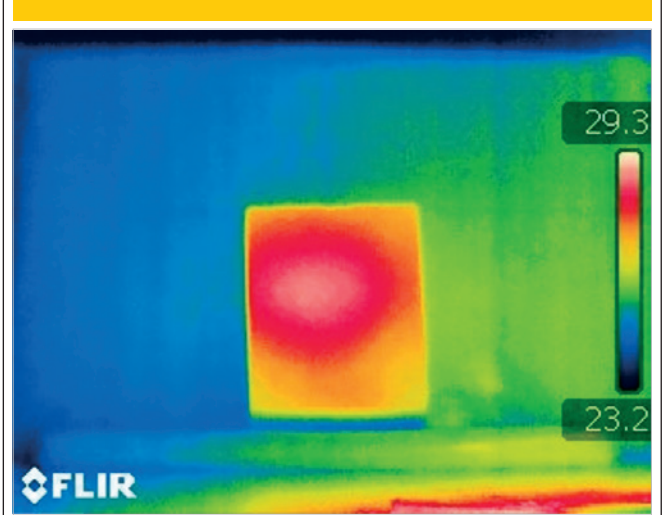Figure 24 – CP1, group 2, height 2 cm

Figure 27 – CP4, group 2, height 5 cm

5.2 Samples of group 2

The results related to samples of group 2 are shown in Figures 24 to 29. In Figure 26, it is noted that from 4 cm mortar thickness (or 5cm total sample height) the image appear less clear than the previous and this lack of clearness has worsened with the increase in mortar layer (or the depth of the damage).

However, it is important to remark that this result is valid only for these experiment conditions: incandescent lamp heating and the time of heating. If the time of heating was increased, for example, one might infer that it should be possible to detect a sample defect located at greater depths. Nonetheless, it does not mean that heating time can be indiscriminately elevated in order to reach the visualization of a greater depth of defect, because an excessive heating can damage the FRP system, impair the adhesion and also the material strength. Summarizing, the excessive heating can weaken and even cancel the structural function of FRP system[17].

5.3 Inserting parameters for the infrared camera

Considering samples of group 1 heated by incandescent lamp, some wrong parameters were purposefully inserted in infrared camera and so the infrared images were compared taking into account their temperatures and the differences between images.

Firstly, the focus was in inserting in the infrared camera greater values of "distance from lens to object" than the ones of the real situation. It is shown in Figure 30 that despite the decrease of temperature values in the point of the defect, it is not possible to assert that this is an effect caused by the insertion of false parameters. The decrease of temperature values also occurs between the first and the last measurement, which have exactly the same parameters inserted. Therefore, this fact might be only due to the natural condition of thermal equilibrium. Thus, if the camera is positioned 1 m distant from the target and if there is an increase of values of "distance from lens to object", there will be no influence in the result of sample temperature when it is measured with the infrared camera.

Figure 31 present the results when considered the 5m real distance (from lens to object).

Once again, it is possible to notice the gradual decrease of temperature between the first and the last measurement which have identical parameters. Thus, also in this case, there will be no
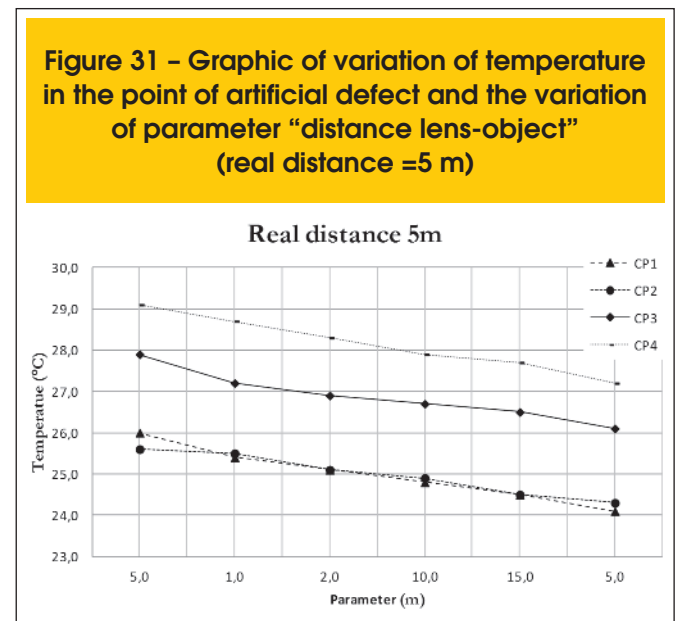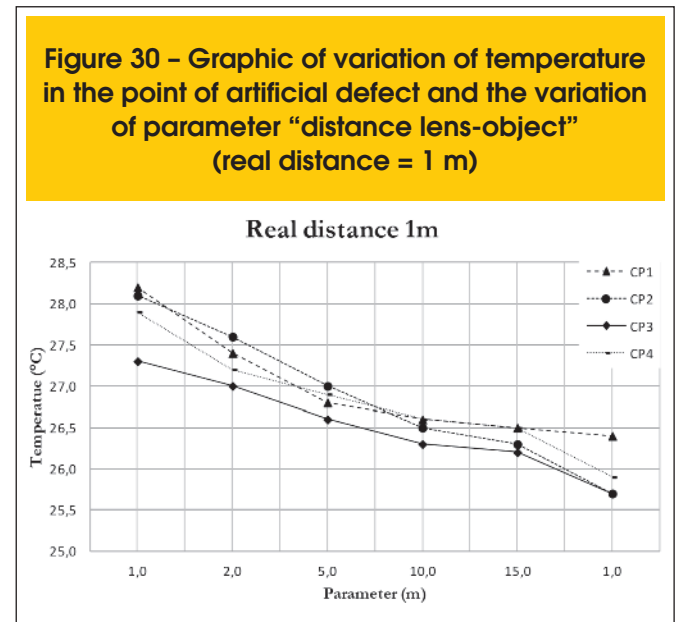

Figure 28 – CP5, group 2, height 6 cm

Figure 30 – Graphic of variation of temperature in the point of artificial defect and the variation of parameter "distance lens-object" (real distance = 1 m)

Figure 29 – CP6, group 2, height 7 cm

Figure 31 – Graphic of variation of temperature in the point of artificial defect and the variation of parameter "distance lens-object" (real distance =5 m)
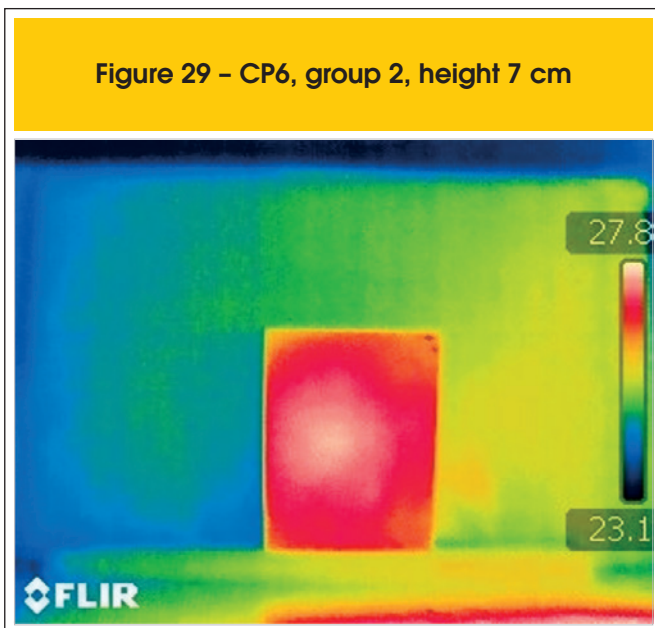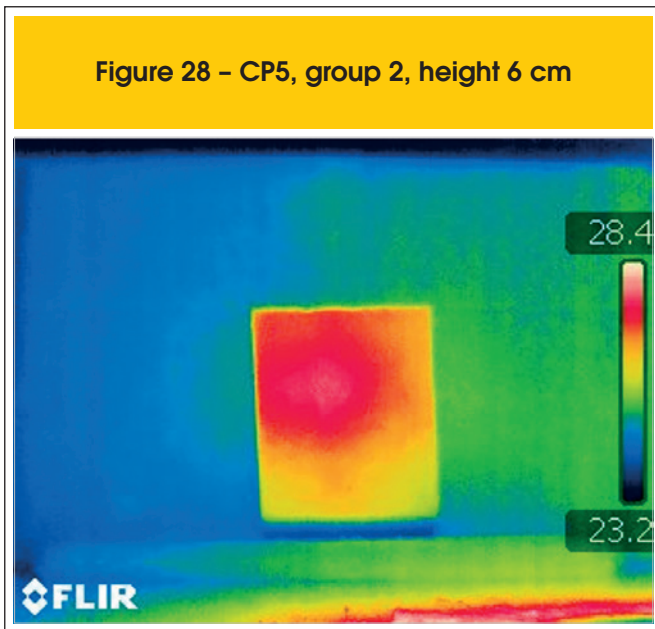
Figure 32 – Graphic of variation of temperature in the point of artificial defect and the variation of parameter "relative air humidity" (real relative air humidity = 64%)

Figure 33 – Graphic of variation of temperature in the point of artificial defect and the variation of parameter "room temperature" (real room temperature = 17°C)
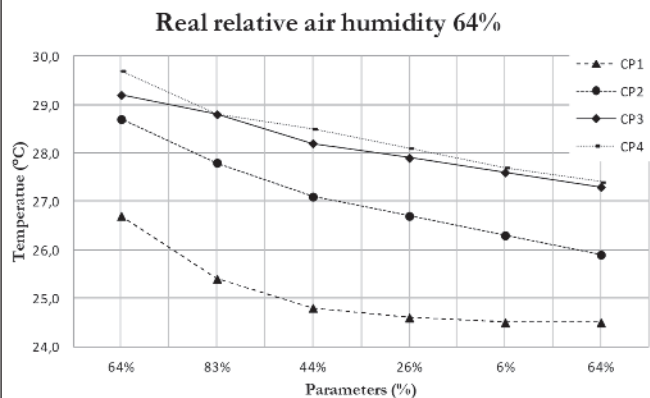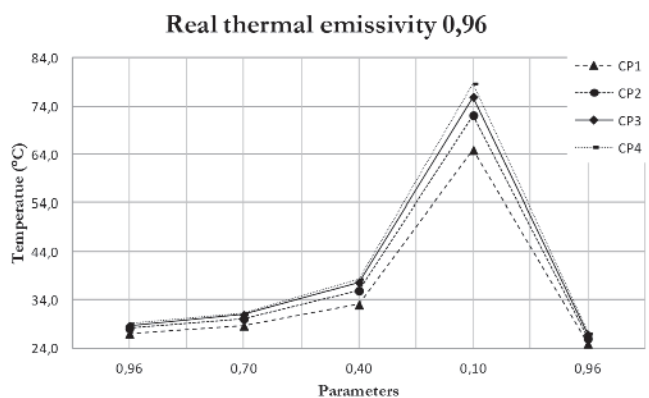

Figure 34 – Graphic of variation of temperature in the point of artificial defect and the variation of parameter of thermal emissivity (real thermal emissivity = 0.96)

influence in the result of sample temperature when the camera is positioned 5 m distant to the target.

Similarly to the previous case, the infrared images also do not present significant contrast differences.

However, if the focus is only in the difference of temperature between samples, it can be noteworthy that, considering 5m distance from lens to object, there is a relation between the size of the defect and temperature: the larger the defect is, the higher the measured temperature in the central point of the defect will be. This is shown in Figure 31.

In Figure 31, the temperature value in the 2cm artificial defect (sample CP2) is very close to the temperature of sample CP1, which have no artificial defect. However, it is noteworthy that the temperature value in 6cm artificial defect (sample CP3) is higher than CP1 (no defect) and CP2 (2cm artificial defect) and lower than CP4 (10 cm defect). The conclusion is that the measurement of temperature of small subsurface damages is impaired when the infrared camera is moved away from the target.

In Figures 32 and 33, the results of variation of parameters of relative humidity and room temperature are respectively shown.

In Figure 32 it is shown that there is an influence if the inserted room temperature is higher than real because there is a small rise in the graphic lines. However, this rises are less than 0.5°C even if the values inserted are very far from real. Thus, the insertion of these false room temperatures can lead to a slight decrease of measurement of temperatures, if compared to real temperatures.

Nonetheless, the influence of relative air humidity (Figure 33) does not present any abnormality of line graphic decay and thus this behaviour can be attributed to the thermal equilibrium.

In Figure 34, is shown that the variation of thermal emissivity has definitely influenced the measurement of temperature when using the infrared camera, because it had a significant increase when the value of thermal emissivity inserted was small.

Form figures 35 and 36 one may infer that the visual detection of damages is not impaired when the thermal emissivity inserted in IR camera is far from the real value.
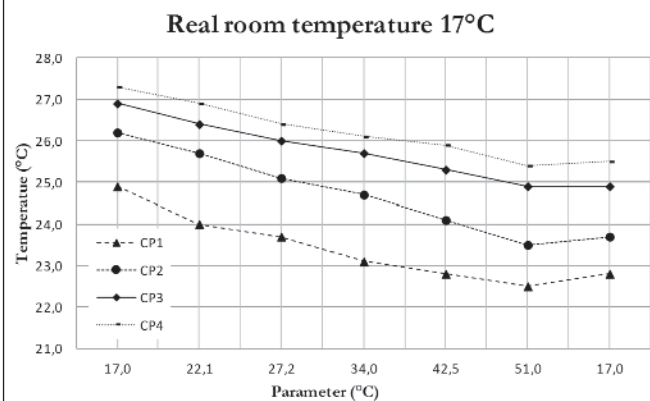
6. Conclusions

Comparing the different types of heating, it is observed that the incandescent lamp is the best device because it allows the identification of the simulated lack of adherence. However, some analysis must be considered if the type of heating is taken into account.

Despite the fact that the incandescent lamp provides clearer infrared images when used as source of heating, its disadvantage is that it consumes too much energy and also that it has poor durability. It does not happen if the high-pressure sodium lamp is used, because the latter is more economic.

Nonetheless, the choice of the heat source depends on how and where the inspection will be performed. If the ambient has

Figure 35 – Infrared images indicating the temperature in the point of the artificial defect when thermal emissivity inserted was 0.96 (1st measurement): (a) CP2, (b) CP3, (c) CP4
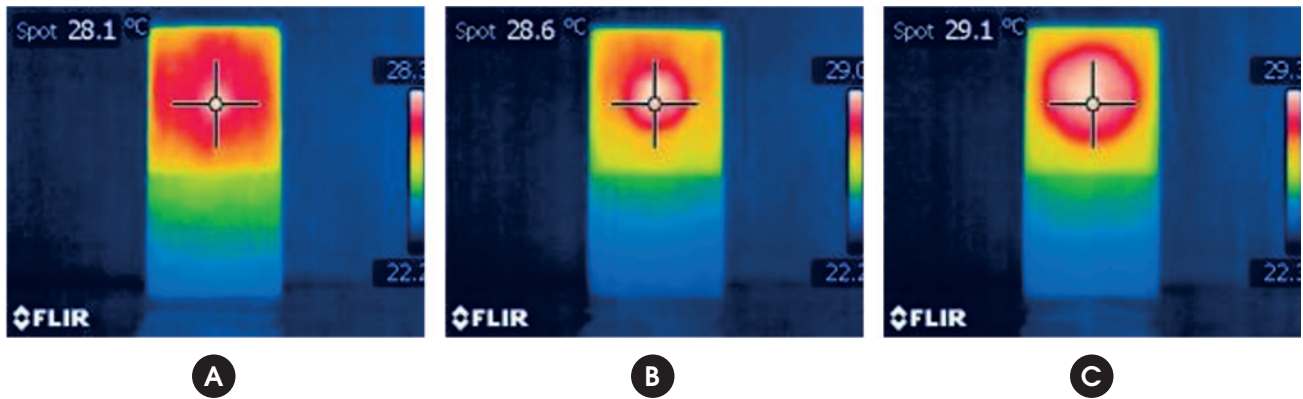
controlled temperature, i.e. constant temperatures, without wind or other heating sources interferences (as in tunnels, for instance), the high-pressure sodium lamp could be the best option. Although the images are less clear than other heat sources, the identification of the defect was noticeable.

According to the experimental work, the results using the convection heater do not demonstrated precision and reliability, unlike those given by the scientific works [7] and [9]. In the later studies the heat flux was controlled, procedure not followed in the present research. This demonstrate that not only the type of heating influences the thermographic evaluation but also how the heat flux will cover the surface of the sample, which is an relevant factor to consider in the analysis.

The individual parameters of "relative air humidity" and "distance from lens to object" do not presented any abnormality neither in the measurement of temperature nor in the distinctness clearness of infrared images. However, the insertion of higher room temperature values can lead to measurements of temperature slightly below the real ones.

The variation of the parameter of thermal emissivity has led to expressive errors when considered temperature measurement and also it has slightly impaired the clearness of the infrared image. These errors were expected because the thermal emissivity is one of the most complex parameters and so it has been studied carefully by some researchers [11][12]. These authors also concluded that the use of incorrect thermal emissivity values could lead to significant errors in the infrared images when the temperature is measured and this lead to misleading interpretations.

In the present paper, it was observed that the visual identification of artificial defect at interface FRP/concrete was not impaired even if the thermal emissivity was far from the real value, once the contour of the polystyrene disc was very visible as it is shown in Figures 35 and 36. Therefore, even if considered an adverse situation, the identification of subsurface damages using infrared thermography as an NDT technique for diagnostic purposes is not invalidated.

A suggestion for future analysis is the study of combined variation of parameters and not only individually, once in field these values

Figure 36 – Infrared images indicating the temperature in the point of the artificial defect when thermal emissivity inserted was 0.1 (4th measurement): (a) CP2, (b) CP3, (c) CP4
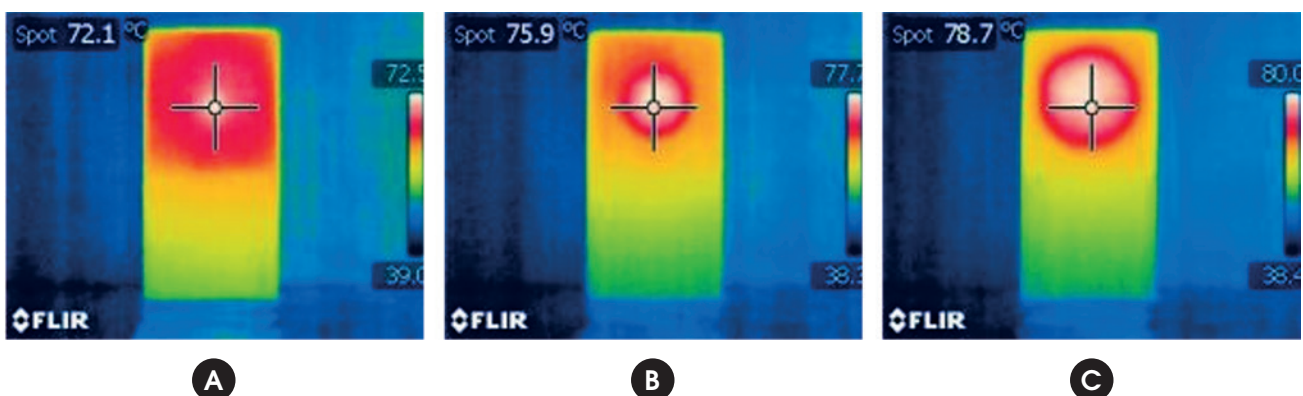
can be varied together. The ongoing research project will consider this factor.

Finally, it is noteworthy that this paper ratifies part of results achieved by other authors who confirm the applicability of the infrared thermography method to verify damages at FRP/concrete interface. It also contributes to new results and indicates the necessity of additional research to clarify some questions raised in the present work.

7. References

[1] Bloch J, Miller K. Bridge to the future?. Bangor Daily News, Bangor, 2009, p.5-7.

[2] Realfonzo R, Martinelli E, Napoli A, Nunziata B. Experimental investigation of the mechanical connection between FRP laminates and concrete. Compos. Part B Eng., v. 45, n. 1, 2013, p. 341–355.

[3] Cho K, Park SY, Kim ST, Cho JR, Kim BS. Shear connection system and performance evaluation of FRP-concrete composite deck. KSCE J. Civ. Eng., v. 14, n. 6, 2010, p. 855–865.

[4] Bengar HA, Maghsoudi AA. Experimental investigations and verification of debonding strain of RHSC continuous beams strengthened in flexure with externally bonded FRPs. Mater. Struct., v. 43, n. 6, 2010, p. 815–837.

[5] Sohn H, Kim SD, In CW, Cronin KE, Harries K. Debonding monitoring of CFRP strengthened RC beams using active sensing and infrared imaging. Smart Struct. Syst., v. 4, n. 4, 2008 pp. 391–406.

[6] Ghosh KK, Karbhari V M. Use of infrared thermography for quantitative non-destructive evaluation in FRP strengthened bridge systems. Mater. Struct., v. 44, n. 1, 2011, p. 169–185.

[7] HALABE, U.B., DUTTA S.S., GANGARAO H.V.S. NDE of FRP Wrapped Colums Using Infrared *In*: Quantitative Non-destructive Evaluation, 34°, 2008, Anais, vol. 975, n. 1, p. 1387–1394.

[8] DUMOLIN J., IBARRA-CASTANEDO C., QUIERTANT M., TAILLADE F., BENDADA A., MALDAGUE X. Evaluation of FRP Gluing on Concrete Structures by Active Infrared Thermography. *In*: Conference on Qualitative InfraRed Thermography, 10°, 2010, pp. 1–9.

[9] DE ALMEIDA E. G. Inspeção Termográfica de Danos por Impacto em Laminados Compósitos Sólidos de Matriz Polimérica Reforçada com Fibras de Carbono, São Carlos, 2010, Dissertação (mestrado)- Universidade de São Paulo, São Carlos, 111 p.

[10] Titman D. Applications of thermography in non-destructive testing of structures. NDT E Int., v. 34, n. 2, 2001, p. 149–154.

[11] MADDING R. P. Emissivity Measurement and Temperature Correction Accurancy Considerations *In*: Thermosense XXI, 21°, 1999, v. 3700, p. 393–401.

[12] RODRÍGUES F. de J. L. Detecção de Defeitos em Materiais Cerâmicos Usando Termografia., Florianópolis, 2010, Dissertação (mestrado) - Universidade Federal de Santa Catarina, 150 p.

[13] Lothenbach B, Winnefeld F. Thermodynamic modelling of the hydration of Portland cement. Cem. Concr. Res., v. 36, 2006, p. 209–226.

[14] SHIN P. H., WEBB S. C., PETERS K. J., "Nondestructive inspection in adhesive-bonded joint CFRP using pulsed phase thermography. *In*: Thermosense: Thermal Infrared Applications XXXV, 35°, 2013, v. 8705, p. 87050Q–1 87050Q–9.

[15] GHIASSI B., SILVA S. M., OLIVEIRA D. V., LOURENÇO P. B., BRAGANÇA L. Assessment of the Bond Quality Degradation in FRP-strengthened Masonry using IR Thermography Technique. *In*: International Symposium on Fiber Reinforcement Polymers for Reinforced Concrete Structures, 11°, Guimarães, 2013, p. 1–9.

[16] Lai WL, Kou SC, Poon CS, Tsang WF, Ng SP, Hung YY. Characterization of Flaws Embedded in Externally Bonded CFRP on Concrete Beams by Infrared Thermography and Shearography. J. Nondestruct. Eval., v. 28, n. 1, 2009, p. 27–35.

[17] M. Robert and B. Benmokrane, "Behavior of GFRP Reinforcing Bars Subjected to Extreme Temperatures," *J. Compos. Constr.*, vol. 14, no. 4, pp. 353–360, 2010.

[18] FLIR Systems, Manual do Utilizador FLIR B series FLIR T series, 2010, p. 274.